Dark energy Constraints from different Local Group Histories

David Benisty[1]

[1] *Frankfurt Institute for Advanced Studies (FIAS), Ruth-Moufang-Strasse 1, 60438 Frankfurt am Main, Germany*[*]

The dynamics of the Local Group (LG), especially concerning the contributions of the Milky Way (MW) and Andromeda (M31) galaxies, is sensitive to the presence of dark energy. This work compares the evolution of the LG by considering it as a two-body problem in a homogeneous and isotropic expanding spacetime, i.e. the McVitte spacetime (McV) versus the spherically symmetric metric for LG dynamics with the Cosmological Constant, i.e. the De Sitter-Schwarzschild spacetime (DsS). Using the Timing Argument (which links LG dynamics to LG mass), calibrated by the IllustrisTNG simulations, we find that the McV spacetime predicts a lower mass for the LG: $(4.20 \pm 0.61) \cdot 10^{12} M_\odot$ for McV spacetime vs. $(4.65 \pm 0.75) \cdot 10^{12} M_\odot$ for DsS spacetime (68%, CL). Due to uncertainties in tangential velocity measurements, the masses are indistinguishable. However, with future astrometric measurements, we demonstrate that the predicted masses will be distinguishable, indicating different LG histories. By independently estimating the total mass of MW and M31, we compare the possible upper bounds for the Cosmological Constant in these scenarios. We find a tighter upper bound for the DsS spacetime model, $\Lambda < 3.3\,\Lambda_{\rm CMB}$, compared to $\Lambda < 8.4\,\Lambda_{\rm CMB}$ for the McV spacetime (where $\Lambda_{\rm CMB}$ is the mean value from Planck). Future astrometric measurements, such as those from JWST, hold the potential to independently detect dark energy for both spacetime models independent from Planck's value.

arXiv:2401.09546v1 [astro-ph.CO] 17 Jan 2024

Introduction - Dark energy (in its simplest form, the Cosmological Constant - Λ) is an unknown type of energy that influences the universe on its largest scales [1]. Its primary impact is to propel the accelerating expansion of the Universe. The first observational evidence for dark energy emerged from supernova measurements [2, 3]. Furthermore, various cosmological observations, such as Baryon Acoustic Oscillations (BAO)[4–7] and the Cosmic Microwave Background (CMB)[8], reinforce the existence of dark energy. Beyond its impact on large scales, dark energy exerts a significant influence on the Local Universe [9–24]. The cosmological constant alters the predicted mass of the LG of galaxies, assuming it primarily comprises of the MW and M31 forming a two-body system [25–37].

That approximate two-body problem can be written as a test body of reduced mass in a gravitational potential embedded in two possible background metric: the DsS and the McV. (i) The DsS metric has a spherical-symmetric form where only Λ drives the expansion: $ds^2 = -(1-\Phi)\,dt^2 + \frac{dr^2}{(1-\Phi)} + r^2 d\Omega^2$ with the potential $\Phi = 2GM/(rc^2) + \Lambda r^2/6$. A test particle in the DsS metric at the low energy limit ($\Phi \ll 1$) obeys the Equation of Motion (EoM):

$$\frac{\ddot{r}}{r} = -\frac{GM}{r^3} + \left(\frac{l}{r^2}\right)^2 + \frac{1}{3}\Lambda c^2, \tag{1}$$

where r is the separation, M is the total mass of the binary system, G is the Newtonian gravitational constant, and c is the speed of light, l is the conserved angular momentum over the reduces mass. (ii) The McV spacetime describes a massive object immersed in an expanding cosmological spacetime [38, 39] and the full Λ Cold Dark Matter model impacts the binary motion. The metric reads: $ds^2 = -(1-\Phi_N)\,dt^2 + \frac{a(t)^2 dr^2}{(1-\Phi_N)} + a(t)^2 r^2\, d\Omega^2$, where $a(t)$ is the scale factor of the Universe and $\Phi_N = 2GM/(rc^2)$. In the low energy limit ($\Phi_N \ll 1$ and $rH \ll 1$) the EoM reads [40–42]:

$$\frac{\ddot{r}}{r} = -\frac{GM}{r^3} + \left(\frac{l}{r^2}\right)^2 + \frac{\ddot{a}}{a}\,. \tag{2}$$

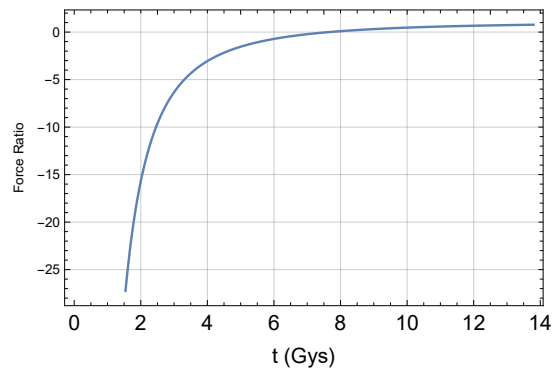

FIG. 1. *The ratio between $\ddot{a}/a$ and $\Lambda c^2/3$ vs. time from $t = 0$ to the age of the Universe, assuming the Λ Cold Dark Matter model. Asymptotically, both ratios approach a constant value. For the $\ddot{a}/a$ case, the expansion rate of the Universe creates an attractive force at early times and only becomes repulsive at late times.*

The main difference between the two descriptions is thus the $\Lambda c^2/3$ vs. $\ddot{a}/a$ term in Eqs. (1) and (2). Fig. (1) shows the ratio between these two contributions over the cosmic time, assuming Λ Cold Dark Matter (ΛCDM) model. While the $\Lambda c^2/3$ remains constant, for $t \approx 7.65_{Gy}$ ($z \approx 0.67$), the $\ddot{a}/a$ acts as an attractive force for early cosmic times.

This work shows that these two different models for the

* benidav@post.bgu.ac.il

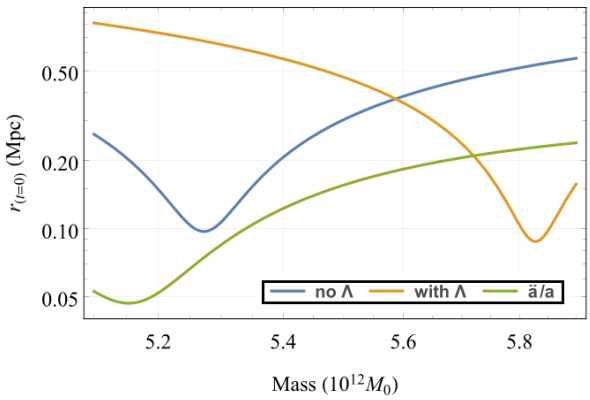

FIG. 2. *The separation of the LG as $t \to 0$ for different masses. The minima of the curves denote the TA masses as can be read off the x-axis.*

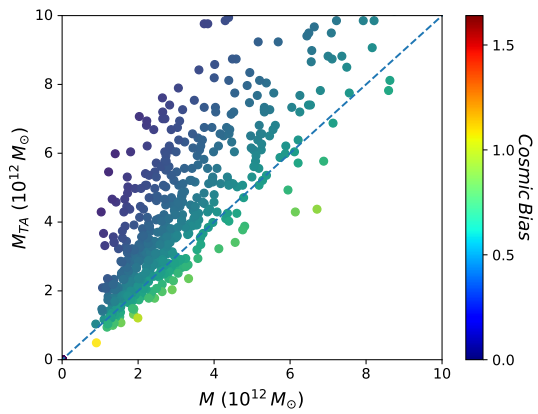

FIG. 3. *The correlation between the Timing Argument mass and the simulation based mass. These chains are selected from the IllustrisTNG cosmological simulation, in which the mass correction factor is computed as the ratio of the actual combined mass of both galaxies to the mass obtained from TA, as described in [31]. The relation shows that the Timing Argument mass is biased biased high w.r.t. the simulated mass. The masses ratio reads $M_{Sim}/M_{TA} = 0.63 \pm 0.02$.*

local cosmic expansion yield different predicted LG mass that will be distinguishable with future measurements such as the James Webb Space Telescope. Thus, only based on the LG masses and dynamics, we will determine which model is suitable to the describe the LG history. Furthermore, we determine the upper bound on Λ based on these two histories and show that with more precise measurements one could detect the Λ contribution to the LG dynamics.

Method - There are different ways to estimate the galaxy masses [24, 35, 36, 43]. The Timing Argument (TA) is a simple way that connects the total mass of the MW and M31 to the kinematics [44–46]. The TA assumes that MW and M31, modelled as point masses, have been approaching each other despite cosmic expansion. Briefly after their formation these two galaxies had minimal separation ($r \to 0$). Since then many modifications of the TA have been proposed, including: (i) the introduction of a Cosmological Constant, which increases the LG mass [34, 37]; (ii) corrections for the effects of hierarchical growth of the two galaxies by comparisons with cosmological simulations [28, 31, 43, 47] which shows the TA is unbiased though suffers from cosmic scatter; (iii) successive refinements of the M31 orbit improving observational accuracy of M31's tangential motion [30, 48–50]. Based on these three modifications we detail the method to predict the LG mass.

(i) For a chosen set of separation and velocities as initial conditions, we numerically solve Eq. (1) or Eq. (2) by integrating backwards in time. Fig. (2) shows the separation of LG-like systems for different background models: purely Newtonian model, adding the Cosmological Constant correction Λ, and the embedding in an expanding Universe $\ddot{a}/a$. The best solution for the minimal separation indicates the TA predicted mass M_{TA}. The predicted TA mass from Λ is higher then the purely Newtonian model since one needs to overcome the repulsion force of Λ via stronger Newtonian attraction. The $\ddot{a}/a$ model yields the lowest mass, since the $\ddot{a}/a$ acts as an attractive force at early times, thus less gravitational attraction (via mass) is needed.

(ii) Given the simplicity of the TA, it is customary to include corrections motivated by galaxy evolution simulations to get unbiased estimates of the true LG mass [28]. The matter has been re-investigated by [31] who uses IllustrisTNG N-body and hydrodynamic simulations. The tendency of the TA is to overestimate the LG mass by a factor of 0.63 ± 0.02. Specifically Ref. [31] identify about 600 bound analogues of the LG by a series of cuts on band magnitude, separation, velocity of approach and total velocity, computing distributions of the Cosmic-Bias. Fig. (3) shows the scatter plot between the TA mass and the simulation-based mass. The TA mass is biased high compared to the simulated mass. To include this modification, we find the closest pair that matches and marginalize the mass over different pairs, via: $M = \int M_{TA}(\theta, \Lambda) P(\theta) d\theta$, where $\theta = (r_0, v_r, v_{\tan})$ are the initial conditions. We assume a Gaussian probability distribution for the different properties of the different LG pairs. For instance, the probability for the separation reads: $P_r \sim \exp \frac{1}{2} \left[(r_0 - \bar{r}_0)/\sigma_r \right]^2$ where r_0 is the separation of the observations and $\bar{r}_0 \pm \sigma_r$ is the mean separation and its standard deviation of the simulated LG pairs.

(iii) The separation of the radial velocity of M31 toward us is known from [30]: $r_0 = 0.77 \pm 0.04\, Mpc$ and $v_r = 109.3 \pm 4.4\, km/sec$ where the uncertainty is very low. However, there are different estimations for the tangential velocities: from $v_{\tan} < 17\, km/sec$ [30], to $57^{+31}_{-35}\, km/sec$ [48] (called **Low** $v_{\tan}$) and the latest estimation $82.4 \pm 31.2\, km/sec$ [49] (called **High** $v_{\tan}$). Ref. [51] shows that higher tangential predicts larger LG mass.

Predicted Local Group Mass - Different EoM and dif-

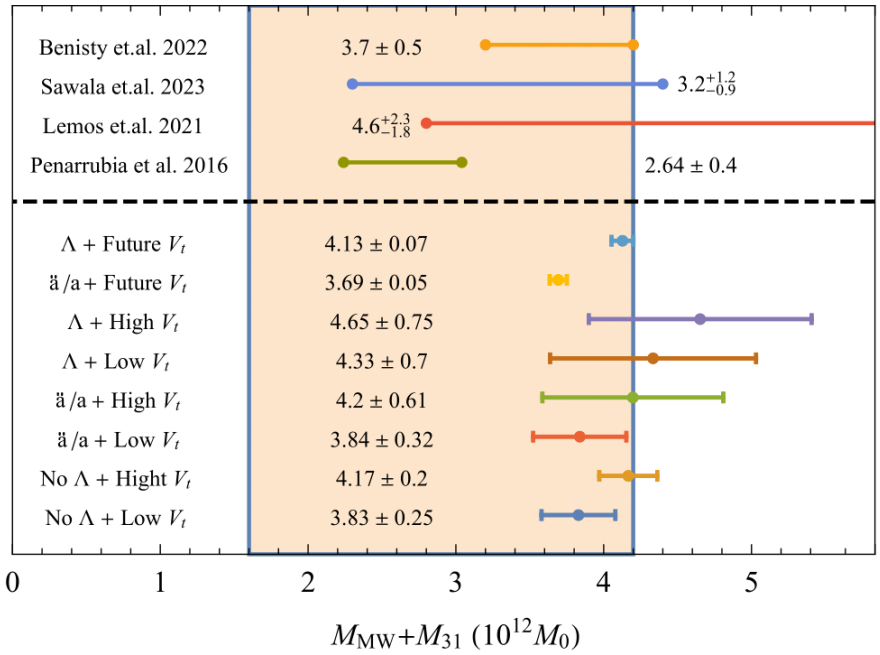

FIG. 4. *The predicted total mass of the Local Group of galaxies based on the proper motion of M31 towards us (Timing Argument) with the simulations calibrations. The figure compares masses inferred from different EoM with $\ddot{a}/a$ vs. pure Λ, with different values of the tangential velocities (**Low** $v_{\mathbf{tan}}$ is $57^{+31}_{-35}\,km/sec$ [48] and **High** $v_{\mathbf{tan}}$ is $82.4 \pm 31.2\,km/sec$ [49]). The figure compares the values with the values from the literature [24, 35, 36, 43]. The orange area shows the uniform range $M_{MW} + M_{31} \in [1.6, 4.2] \cdot 10^{12}\,M_\odot$ that on complementary masses estimates [35].*

ferent histories yield different LG masses. Fig. (4) shows the different predicted masses for the different histories. The $\ddot{a}/a$ model gives the lowest mass and the Λ repulsion force model requires the largest mass. Another effect that changes the mass is the tangential velocity. The **High** $v_{\mathbf{tan}}$ gives higher masses than the masses based on the **Low** $v_{\mathbf{tan}}$. Due to the large uncertainties in the tangential velocities, the different masses are not distinguishable. In earlier studies we assumed the cosmic bias to have a major impact on the mass, but in this study we show that the most significant effect comes from the tangential velocity. The impact of the Cosmic Bias based on our simulations is less significant than the uncertainty of tangential velocity, since the uncertainty of the Cosmic Bias is lower. By assuming 5% uncertainty for the tangential velocity with the mean value of $50\,km/sec$, we find that the two different predicted masses have a $\sim 5.8\sigma$ difference which shows they are distinguishable and separable.

There are several values for the separate masses of each galaxy in the literature. Given the different values for the LG masses, we take a number of estimates of each mass obtained through different methods, and assume that the true value is contained within the ranges of the different estimates. As [35] estimates, the mass of the MW reads: $M_{MW} \in [1, 2.2] \cdot 10^{12}\,M_\odot$, and the M31 mass reads: $M_{31} \in [0.6, 2.0] \cdot 10^{12}\,M_\odot$, based on [52–61]. Combining these two measurements yields the prior: $M_{LG} \in [1.6, 4.2] \cdot 10^{12}\,M_\odot$. Fig. (4) shows the possible estimated total masses (the orange area). From our estimations and with other estimations from the literature seems very likely that the Local Group mass is dominated by its two most massive member galaxies, as other Ref. [62] conclude. Increasing the measurement precision for the tangential velocity, a high value can be distinguished from a low one. As Fig. (4) shows, increasingly high tangential velocities may lead to LG masses outside the orange area and thus disagreeing with estimates from the literature. This could create an interesting tension between the LG estimated masses.

History and Future - The predicted LG masses give the opportunity to evaluate the history and the future of the LG. Ref. [63] discusses the effect of $\ddot{a}/a$ with dynamical friction. Here we use the TA with the simulation calibration without additional effects and defer further effects to future research. The upper panel of Fig. (5) shows the past of the M31 separation vs. time (solid line) and the future motion towards us (dashed line). The masses that we introduce are the masses with the simulation calibration and therefore could deviate from the TA initial condition ($r = 0$ for $t = 0$). The numerical solution in Fig. (5) shows that the $\ddot{a}/a$ is more compatible with the TA initial condition, even with the simulation calibration while the Λ expansion model gives an initial separation similar to the current one.

Bounds on dark energy - Large values of the Cosmological Constant require LG masses that are too large to be compatible with existing estimates from complemen-

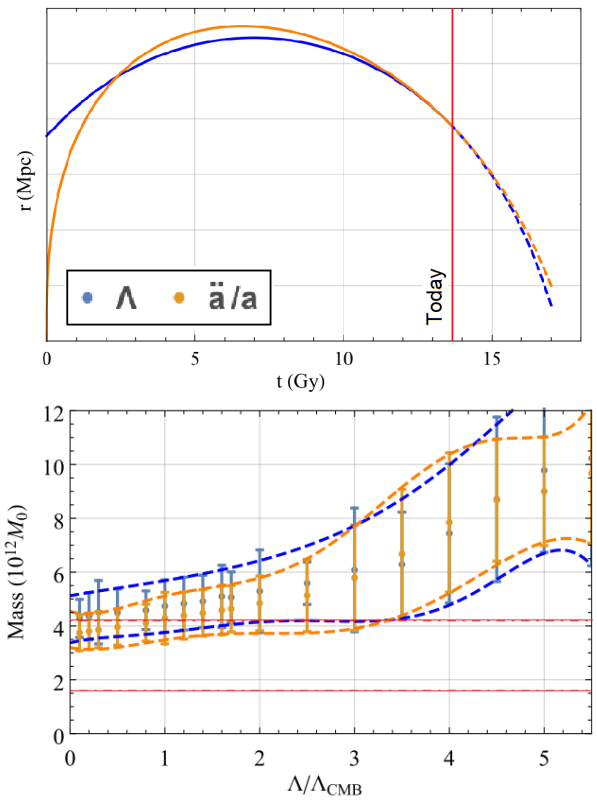

FIG. 5. ***Upper:*** *The orbital evolution for the MW and M31 is shown from $t = 0$ until today with solid lines, and for the future with dashed lines. For the pure Λ model the line is plotted in blue and for the $\ddot{a}/a$ model in orange.* ***Lower:*** *The predicted mass of the LG for different values of dark energy, using the Timing Argument and the simulations calibration, for the Λ vs. $\ddot{a}/a$ models. Pure Λ repulsion force gives higher LG mass. For large Λ, the predicted LG mass becomes be too large. Based on the uniform range $M_{MW} + M_{31} \in [1.6, 4.2] \cdot 10^{12}\, M_\odot$ (red lines) we obtain the upper bounds on Λ from the different histories.*

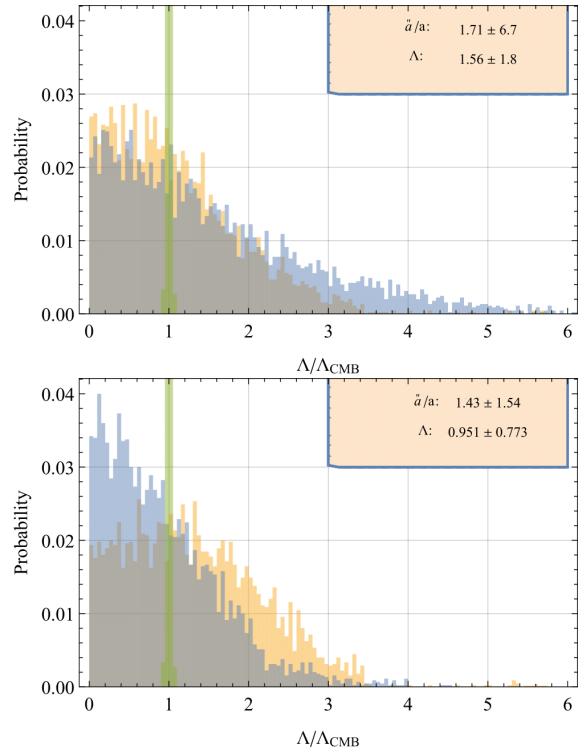

FIG. 6. *Constraints on dark energy based on the LG kinematics for the $\ddot{a}/a$ (blue) vs. Λ (orange) models for the local cosmic expansions with the* ***High*** $v_{\mathbf{tan}}$ *is 82.4 ± 31.2 km/sec [49]. The upper panel shows the current tangential velocity statistics, and the lower panel shows the possible future tangential velocity statistics with 5% error. The value of the Cosmological Constant from Planck is presented in green. The mean and variance values of the Λ distribution are written on the panels of the figures (with $\Lambda > 0$), where $\ddot{a}/a$ is the McV repulsion force and the Λ is the SdS repulsion force.*

tary data, that served as the uniform mass prior. The upper panel of Fig. (5) shows the predicted mass of the LG of galaxies for different values of dark energy, using the Timing Argument and the simulations calibration, for the Λ vs. $\ddot{a}/a$ models. The prior of the known masses is presented as red dashed lines. For certain values of Λ the predicted mass in biased high. To infer the Λ value based on the LG estimated masses, we generate a uniform prior for the LG masses and independently a Gaussian prior for the separation and the velocities. For each mass and initial conditions θ, we extract the TA mass and by extrapolate backwards in time (to fulfill the condition $r \to 0$ for $t = 0$), we determine the corresponding Λ value. Formally the Λ distribution reads: $P(\Lambda) = \int P(M)P(\theta)dM\, d\theta$, with $\theta = (r_0, v_t, v_t)$. Fig. (6) shows the constraints on dark energy for the $\ddot{a}/a$ (blue) vs. Λ (orange) models. The value of the Cosmological Constant from Planck is presented in green. The upper panel shows the **high** $v_{\mathbf{tan}}$ distribution. The values are written on the plot, which gives $\Lambda < 8.4\Lambda_{\rm CMB}$ for the $\ddot{a}/a$ model and $\Lambda < 3.3\Lambda_{\rm CMB}$ for the Λ local dynamical model, where we define the upper bound by the $1-\sigma$ interval of the statistics. The upper bound on Λ from the $\ddot{a}/a$ model is much higher, since the $\ddot{a}/a$ model predicts lower masses than the Λ model. In this way, for the same prior mass, the predicted Λ from $\ddot{a}/a$ is free to be higher. The lower panel shows the possible future tangential velocity statistics with 5% error. The values of the Λ distribution are written on the panels of the figures: $\Lambda < 2.93\,\Lambda_{\rm CMB}$ for the $\ddot{a}/a$ model and $\Lambda < 1.72\,\Lambda_{\rm CMB}$ for the Λ model. Given the small 1σ interval, this will be a direct detection of dark energy for the SdS (at 68%CL).

Discussion - Binary motion can be embedded in different spacetimes. The De-Sitter Schwarzschild (DsS) spacetime contains the Cosmological Constant as a linear repulsion force $\Lambda c^2 r/3$ and assumes spherical symmetry. The McVittie (McV) spacetime combines the DsS and the Friedmann Universe to produce a new spherically symmetric metric that describes a point mass embedded in an expanding Universe. The repulsion force of the McV metric reads $\ddot{a}/a \cdot r$ that behaves as an attractive

force at early times and asymptotically approaches DsS $\Lambda c^2 r/3$ solution. This work discusses which spacetime is suitable to describe the LG motion (as an approximate binary motion dominated by the MW and M31). As a result, it is found that the different spacetimes yield different LG masses that with the JWST data will be distinguishable. The question whether the McV or the DsS spectimes is the most compatible description for our local Universe is related to the fundamental problem to probe the homogeneous and isotropic background cosmology at the small non-linear scales [64]. Using the TA calibrated by the IllustrisTNG simulations, we find that the McV spacetime predicts a lower mass for the LG: $(4.20 \pm 0.61) \cdot 10^{12} M_\odot$ for McV spacetime than $(4.65 \pm 0.75) \cdot 10^{12} M_\odot$ for DsS spacetime. Due to uncertainties in tangential velocity measurements, the masses are indistinguishable. However, with future astrometric measurements from JWST we demonstrate that the predicted masses will be distinguishable and they indicate different LG histories.

To complete our discussion, we use independent measurements for the LG mass (assuming the total mass to be approximated by the sum of masses for MW and M31) in order to calibrate the value of the Cosmological Constant. We obtain $\Lambda < 8.4\,\Lambda_{\rm CMB}$ for the $\ddot{a}/a$ model and $\Lambda < 3.3\Lambda_{\rm CMB}$ for the Λ local dynamical model. The upper bound on Λ from the $\ddot{a}/a$ model is much higher, since the $\ddot{a}/a$ model predicts lower masses than the Λ. In this way, for the same prior mass, the predicted Λ from $\ddot{a}/a$ is free to be higher. With future JWST data (and the COSMICFLOW data [65, 66]) the constraint is expected to improve: $\Lambda < 2.97\,\Lambda_{\rm CMB}$ for the $\ddot{a}/a$ model and $\Lambda < 1.72\,\Lambda_{\rm CMB}$ for the Λ model. For the Λ model it will be a direct detection for dark energy independent from Planck. This opens a new direction to investigate the nature of dark energy at small scales because it allows us to determine when a constant Λ term is sufficient to represent external repulsion in binary systems and when we have to take into account a temporal evolution of the external embedding. Being able to constrain $\Lambda > 0$ for increased measurement precision will also be important to finally conclude that the influence of neighbouring masses, i.e. Cosmic Bias, cannot account for the total repulsion and cosmic expansion has an impact on binary systems.

Acknowledgments - DB thanks the Carl-Wilhelm Fueck Stiftung and the Margarethe und Herbert Puschmann Stiftung. DB thanks to Jenny Wagner and Eduardo Guendelman for useful comments and discussions. DB has received partial support from European COST action CA21136.

[1] P. J. E. Peebles and B. Ratra, Rev. Mod. Phys. **75**, 559 (2003), arXiv:astro-ph/0207347.
[2] S. Perlmutter *et al.* (Supernova Cosmology Project), Astrophys. J. **517**, 565 (1999), arXiv:astro-ph/9812133.
[3] D. M. Scolnic *et al.* (Pan-STARRS1), Astrophys. J. **859**, 101 (2018), arXiv:1710.00845 [astro-ph.CO].
[4] G. E. Addison, G. Hinshaw, and M. Halpern, Mon. Not. Roy. Astron. Soc. **436**, 1674 (2013), arXiv:1304.6984 [astro-ph.CO].
[5] E. Aubourg *et al.*, Phys. Rev. D **92**, 123516 (2015), arXiv:1411.1074 [astro-ph.CO].
[6] A. J. Cuesta, L. Verde, A. Riess, and R. Jimenez, Mon. Not. Roy. Astron. Soc. **448**, 3463 (2015), arXiv:1411.1094 [astro-ph.CO].
[7] A. Cuceu, J. Farr, P. Lemos, and A. Font-Ribera, JCAP **10**, 044 (2019), arXiv:1906.11628 [astro-ph.CO].
[8] N. Aghanim *et al.* (Planck), Astron. Astrophys. **641**, A6 (2020), [Erratum: Astron.Astrophys. 652, C4 (2021)], arXiv:1807.06209 [astro-ph.CO].
[9] A. Chernin, P. Teerikorpi, and Y. Baryshev, (2000), arXiv:astro-ph/0012021.
[10] Y. Baryshev, A. Chernin, and P. Teerikorpi, (2000), arXiv:astro-ph/0011528.
[11] A. D. Chernin, D. I. Santiago, and A. S. Silbergleit, Phys. Lett. A **294**, 79 (2002), arXiv:astro-ph/0106144.
[12] Y. J. Kim, J. Kang, M. G. Lee, and I. S. Jang, Astrophys. J. **905**, 104 (2020), arXiv:2010.01364 [astro-ph.CO].
[13] I. D. Karachentsev, A. D. Chernin, and P. Teerikorpi, Astrofiz. **46**, 399 (2003), arXiv:astro-ph/0304250.
[14] A. D. Chernin, I. D. Karachentsev, M. J. Valtonen, V. P. Dolgachev, L. M. Domozhilova, and D. I. Makarov, Astron. Astrophys. **415**, 19 (2004), arXiv:astro-ph/0310048.
[15] P. Teerikorpi, A. D. Chernin, and Y. V. Baryshev, Astron. Astrophys. **440**, 791 (2005), arXiv:astro-ph/0506683.
[16] A. D. Chernin, P. Teerikorpi, M. J. Valtonen, G. G. Byrd, V. P. Dolgachev, and L. M. Domozhilova, (2009), arXiv:0902.3871 [astro-ph.CO].
[17] A. D. Chernin, P. Teerikorpi, and Y. V. Baryshev, Astron. Astrophys. **456**, 13 (2006), arXiv:astro-ph/0603226.
[18] S. Peirani and J. A. D. F. Pacheco, Astron. Astrophys. **488**, 845 (2008), arXiv:0806.4245 [astro-ph].
[19] A. D. Chernin, I. D. Karachentsev, O. G. Nasonova, P. Teerikorpi, M. J. Valtonen, V. P. Dolgachev, L. M. Domozhilova, and G. G. Byrd, Astron. Astrophys. **520**, A104 (2010), arXiv:1006.0555 [astro-ph.CO].
[20] P. Teerikorpi and A. D. Chernin, Astron. Astrophys. **516**, A93 (2010), arXiv:1006.0066 [astro-ph.CO].
[21] A. D. Chernin, Astron. Rep. **59**, 474 (2015).
[22] A. D. Chernin, N. V. Emelyanov, and I. D. Karachentsev, Mon. Not. Roy. Astron. Soc. **449**, 2069 (2015), arXiv:1508.03485 [astro-ph.CO].
[23] A. Silbergleit and A. Chernin, *Kepler Problem in the Presence of Dark Energy, and the Cosmic Local Flow*, SpringerBriefs in Physics (Springer, 2019).
[24] D. Benisty, J. Wagner, and D. Staicova, (2023), arXiv:2310.11488 [astro-ph.CO].
[25] N. V. Emelyanov, M. Y. Kovalyov, and A. D. Chernin, Astronomy Reports **59**, 510 (2015).
[26] E. Carlesi, Y. Hoffman, J. G. Sorce, and S. Got-

tlöber, Mon. Not. Roy. Astron. Soc. **465**, 4886 (2017), arXiv:1611.08078 [astro-ph.GA].
[27] R. E. Gonzalez, A. V. Kravtsov, and N. Y. Gnedin, Astrophys. J. **793**, 91 (2014), arXiv:1312.2587 [astro-ph.CO].
[28] Y.-S. Li and S. D. M. White, Mon. Not. Roy. Astron. Soc. **384**, 1459 (2008), arXiv:0710.3740 [astro-ph].
[29] A. D. Chernin, I. D. Karachentsev, P. Teerikorpi, M. J. Valtonen, G. G. Byrd, Y. N. Efremov, V. P. Dolgachev, L. M. Domozhilova, D. I. Makarov, and Y. V. Baryshev, Grav. Cosmol. **16**, 1 (2010), arXiv:0706.4068 [astro-ph].
[30] R. P. van der Marel, M. Fardal, G. Besla, R. L. Beaton, S. T. Sohn, J. Anderson, T. Brown, and P. Guhathakurta, Astrophys. J. **753**, 8 (2012), arXiv:1205.6864 [astro-ph.GA].
[31] O. V. Hartl and L. E. Strigari, Mon. Not. Roy. Astron. Soc. **511**, 6193 (2022), arXiv:2107.11490 [astro-ph.CO].
[32] S. Phelps, A. Nusser, and V. Desjacques, Astrophys. J. **775**, 102 (2013), arXiv:1306.4013 [astro-ph.CO].
[33] M. McLeod, N. Libeskind, O. Lahav, and Y. Hoffman, JCAP **12**, 034 (2017), arXiv:1606.02694 [astro-ph.GA].
[34] C. Partridge, O. Lahav, and Y. Hoffman, Mon. Not. Roy. Astron. Soc. **436**, 45 (2013), arXiv:1308.0970 [astro-ph.CO].
[35] P. Lemos, N. Jeffrey, L. Whiteway, O. Lahav, N. I. Libeskind, and Y. Hoffman, Phys. Rev. D **103**, 023009 (2021), arXiv:2010.08537 [astro-ph.GA].
[36] J. Peñarrubia, Y.-Z. Ma, M. G. Walker, and A. McConnachie, Mon. Not. Roy. Astron. Soc. **443**, 2204 (2014), arXiv:1405.0306 [astro-ph.GA].
[37] D. Benisty, A.-C. Davis, and N. W. Evans, Astrophys. J. Lett. **953**, L2 (2023), arXiv:2306.14963 [astro-ph.CO].
[38] G. C. McVittie, Mon. Not. R. Astron. Soc. **93**, 325 (1933).
[39] N. Kaloper, M. Kleban, and D. Martin, Phys. Rev. D **81**, 104044 (2010), arXiv:1003.4777 [hep-th].
[40] M. Sereno and P. Jetzer, Phys. Rev. D **75**, 064031 (2007), arXiv:astro-ph/0703121.
[41] V. Faraoni and A. Jacques, Phys. Rev. D **76**, 063510 (2007), arXiv:0707.1350 [gr-qc].
[42] R. Nandra, A. N. Lasenby, and M. P. Hobson, Mon. Not. Roy. Astron. Soc. **422**, 2931 (2012), arXiv:1104.4447 [gr-qc].
[43] T. Sawala, J. Peñarrubia, S. Liao, and P. H. Johansson, Mon. Not. Roy. Astron. Soc. **526**, L77 (2023), arXiv:2307.13732 [astro-ph.CO].
[44] F. D. Kahn and L. Woltjer, Astrophys. J. **130**, 705 (1959).
[45] D. Lynden-Bell, The Observatory **101**, 111 (1981).
[46] S. Raychaudhury and D. Lynden-Bell, Mon. Not. R. Astron. Soc. **240**, 195 (1989).
[47] T. L. Kroeker and R. G. Carlberg, Astrophys. J. **376**, 1 (1991).
[48] R. P. van der Marel, M. A. Fardal, S. T. Sohn, E. Patel, G. Besla, A. del Pino, J. Sahlmann, and L. L. Watkins, Astrophys. J. **872**, 24 (2019), arXiv:1805.04079 [astro-ph.GA].
[49] J. B. Salomon, R. Ibata, C. Reylé, B. Famaey, N. I. Libeskind, A. W. McConnachie, and Y. Hoffman, Mon. Not. R. Astron. Soc. **507**, 2592 (2021), arXiv:2012.09204 [astro-ph.GA].
[50] K. Chamberlain, A. M. Price-Whelan, G. Besla, E. C. Cunningham, N. Garavito-Camargo, J. Peñarrubia, and M. S. Petersen, Astrophys. J. **942**, 18 (2023), arXiv:2204.07173 [astro-ph.GA].
[51] D. Benisty, E. Vasiliev, N. W. Evans, A.-C. Davis, O. V. Hartl, and L. E. Strigari, Astrophys. J. Lett. **928**, L5 (2022), arXiv:2202.00033 [astro-ph.GA].
[52] J. D. Diaz, S. E. Koposov, M. Irwin, V. Belokurov, and N. W. Evans, Mon. Not. Roy. Astron. Soc. **443**, 1688 (2014), arXiv:1405.3662 [astro-ph.GA].
[53] D. Zaritsky and H. Courtois, Mon. Not. Roy. Astron. Soc. **465**, 3724 (2017), arXiv:1611.04574 [astro-ph.GA].
[54] K. Hattori, M. Valluri, E. F. Bell, and I. U. Roederer, Astrophys. J. **866**, 121 (2018), arXiv:1805.03194 [astro-ph.GA].
[55] L. Posti and A. Helmi, Astron. Astrophys. **621**, A56 (2019), arXiv:1805.01408 [astro-ph.GA].
[56] L. L. Watkins, R. P. van der Marel, S. T. Sohn, and N. W. Evans, Astrophys. J. **873**, 118 (2019), arXiv:1804.11348 [astro-ph.GA].
[57] E. V. Karukes, M. Benito, F. Iocco, R. Trotta, and A. Geringer-Sameth, J. Cosmol. Astropart. Phys. **2020**, 033 (2020), arXiv:1912.04296 [astro-ph.GA].
[58] E. Corbelli, S. Lorenzoni, R. A. M. Walterbos, R. Braun, and D. A. Thilker, Astron. Astrophys. **511**, A89 (2010), arXiv:0912.4133 [astro-ph.CO].
[59] A. Tamm, E. Tempel, P. Tenjes, O. Tihhonova, and T. Tuvikene, Astron. Astrophys. **546**, A4 (2012), arXiv:1208.5712 [astro-ph.CO].
[60] P. R. Kafle, S. Sharma, G. F. Lewis, A. S. G. Robotham, and S. P. Driver, Mon. Not. Roy. Astron. Soc. **475**, 4043 (2018), arXiv:1801.03949 [astro-ph.GA].
[61] J. Peñarrubia, F. A. Gómez, G. Besla, D. Erkal, and Y.-Z. Ma, Mon. Not. Roy. Astron. Soc. **456**, L54 (2016), arXiv:1507.03594 [astro-ph.GA].
[62] T. Sawala, M. Teeriaho, and P. H. Johansson, Mon. Not. Roy. Astron. Soc. **521**, 4863 (2023), arXiv:2210.07250 [astro-ph.GA].
[63] M. Eingorn, A. Kudinova, and A. Zhuk, JCAP **04**, 010 (2013), arXiv:1211.4045 [astro-ph.CO].
[64] P. K. Aluri *et al.*, Class. Quant. Grav. **40**, 094001 (2023), arXiv:2207.05765 [astro-ph.CO].
[65] H. M. Courtois, D. Pomarede, R. B. Tully, and D. Courtois, Astron. J. **146**, 69 (2013), arXiv:1306.0091 [astro-ph.CO].
[66] R. B. Tully *et al.*, Astrophys. J. **944**, 94 (2023), arXiv:2209.11238 [astro-ph.CO].